Available online at www.sciencedirect.com
SCIENCE DIRECT
Vision Research 46 (2006) 2298–2309
Vision Research
www.elsevier.com/locate/visres

Visual summation in night-flying sweat bees: A theoretical study

Jamie Carroll Theobald [a,*,1], Birgit Greiner [a], William T. Wcislo [b], Eric J. Warrant [a]

[a] Department of Cell and Organism Biology, Helgonavägen 3, Lund University, S-223 62, Lund, Sweden
[b] Smithsonian Tropical Research Institute, Box 0843-03092, Balboa, Ancon, Panama

Received 31 October 2005; received in revised form 25 December 2005

Abstract

Bees are predominantly diurnal; only a few groups fly at night. An evolutionary limitation that bees must overcome to inhabit dim environments is their eye type: bees possess apposition compound eyes, which are poorly suited to vision in dim light. Here, we theoretically examine how nocturnal bees *Megalopta genalis* fly at light levels usually reserved for insects bearing more sensitive superposition eyes. We find that neural summation should greatly increase *M. genalis*'s visual reliability. Predicted spatial summation closely matches the morphology of laminal neurons believed to mediate such summation. Improved reliability costs acuity, but dark adapted bees already suffer optical blurring, and summation further degrades vision only slightly.

Keywords: Nocturnal vision; Noise; Neural summation; Apposition compound eyes; Halictid bees

1. Introduction

The nocturnal halictid bees, *Megalopta genalis* are native to neotropical forests where they nest in hollowed out sticks (for example: Arneson & Wcislo, 2003; Janzen, 1968; Wcislo et al., 2004). Quite unlike most bees, *M. genalis* leave to forage during only two time windows each day: shortly after sunset, and shortly before sunrise (Kelber et al., 2006; Warrant et al., 2004), when thick forest canopies and the quick onset of darkness at tropical latitudes force them to be active in profound darkness—about 20 times dimmer than starlight. These bees nonetheless survey the visual scene when they leave the nest, fly off to forage, and return again to the nest entrance of an inconspicuous stick hidden among the trees. Remarkably, they use remembered visual landmarks to guide this flight to the nest (Warrant et al., 2004).

Vision depends on light capture, so vision in dim light, where there is little light energy, is problematic (recently reviewed by Warrant, 2004). The visual signal is faint, because energy is low, and it is noisy, because this energy is absorbed only in random and discrete packets of photons. These factors result in a signal-to-noise ratio that drops with light level. This is described by the DeVries-Rose law: signal-to-noise ratio scales with the square root of mean photon capture (De Vries, 1943; Pelli, 1990; Rose, 1942). Under darkness, when few photons are available, photoreceptors operate with a low signal-to-noise ratio. For vision in dim light, the DeVries-Rose law describes performance well (Hess, 1990; Howard & Snyder, 1983; Laughlin, 1981b, 1990; Shapley & Enroth-Cugell, 1984; Sharpe, 1990).

Because photon noise limits the statistical reliability of photon sampling, the remedy is to increase sample size, and the simplest route is larger eyes and more sensitive optics. Insects are constrained by their own size and the energetic considerations of flight, which restricts the maximum eye size attainable. Nevertheless, female *M. genalis* have large eyes for their body size (Jander & Jander, 2002). Superposition eyes are the design typical of nocturnal insects, such as moths and beetles. They confer some of the benefits of larger lenses by gathering light through many adjacent facets for each rhabdom. However, all bees,

* Corresponding author. Fax: +46 46 222 4425.
E-mail address: Jamie.Theobald@cob.lu.se (J.C. Theobald).
[1] Supported by the National Science Foundation (USA), International Research Fellowship Program.

0042-6989/$ - see front matter © 2006 Elsevier Ltd. All rights reserved.
doi:10.1016/j.visres.2006.01.002

have apposition eyes, in which only one facet gathers light for each rhabdom. Still, *M. genalis* maximize light collection with other optical and retinal adaptations: compared with diurnal halictid bees, facet lenses are 1.8 times larger, and rhabdoms are 4–5 times wider (Greiner, Ribi, & Warrant, 2004a). But these modifications increase sensitivity by only 27 times (Greiner et al., 2004a)—a substantial gain over diurnal bees, but nowhere near enough to account for the eight orders of magnitude less light under which *M. genalis* fly.

Signal-to-noise ratio can be further improved in dim light by neural strategies—summing the outputs of neighboring visual channels (spatial summation) or increasing the visual integration time (temporal summation). These are roughly analogous to a photographer using coarser films or longer exposures to compensate for low light. In both cases summation comes at the cost of acuity (spatial and temporal resolution) but visual performance in dim light can nonetheless be dramatically improved, especially in small eyes like those found in insects (Warrant, 1999; Warrant, Porombka, & Kirchner, 1996). Further, anatomical evidence from the first optic ganglion (lamina) of *M. genalis* strongly suggests that spatial summation might be mediated by wide laterally spreading first-order interneurons (L-fibers) (Greiner, Ribi, Wcislo, & Warrant, 2004b; Greiner, Ribi, & Warrant, 2005).

Our goal was to model the visual system of *M. genalis* and simulate the effect of summation on visual performance. By setting spatial and temporal summation as parameters to be optimized, we examined to what degree and under what circumstances summation would benefit a bee. One major question to be answered by the modeling is as follows: at the light intensities and image velocities normally encountered by these bees, does the number of cartridges (visual units within the lamina) predicted to be required for spatial summation agree with the number of cartridges actually visited by the L-fibers? Such an agreement would strengthen our hypothesis that the L-fibers are involved in spatial summation and thus improve visual performance at night.

2. Theory and methods

2.1. A model of spatiotemporal summation

The effect of spatial and temporal summation on visual performance in *M. genalis* was theoretically determined using a model to calculate the finest spatial frequency that an eye can reliably see at a given light intensity (I) and image velocity (v). A convenient benchmark for this is signal-to-noise ratio of 1.0, the point where signal and noise have equal power in an image. For our purposes, the level at which signal and noise are equal gives the maximum detectable spatial frequency ($v_{\max}$) (Warrant et al., 1996; Warrant, 1999), which is

$$v_{\max} = \frac{0.530}{\Delta\rho_T}\sqrt{\ln(mN) - \frac{1}{2}\ln[N + \sigma_D^2]}, \tag{1}$$

where m is the contrast of the image (taken as 0.4, interpolated from data in (Laughlin, 1981a), N is the total number of photons sampled by a visual channel during Δt, one integration time, σ_D^2 is the total dark variance (due to thermally induced photopigment isomerisations), and $\Delta\rho_T$ is the half-width of the Gaussian spatial receptive field resulting from spatial and temporal summation (Fig. 1). These parameters depend on whether or not spatiotemporal summation is being considered, and are given by (Warrant et al., 1996; Warrant, 1999):

$$N = 0.890\Delta\rho^2 D^2 \Delta t \int \kappa\tau(1 - e^{-kR_i(\lambda)I})I(\lambda)d\lambda \quad \text{(no summation)} \tag{2a}$$

$$= 1.269\left(\frac{\Delta\rho_p}{\Delta\phi}\right)^2 \Delta\rho^2 D^2 \Delta t \int \kappa\tau(1 - e^{-kR_i(\lambda)I})I(\lambda)d\lambda \quad \text{(summation)} \tag{2b}$$

$$\sigma_D^2 = 0.785\omega l \Delta t d^2 \quad \text{(no summation)} \tag{3a}$$

$$= 1.131\omega l \Delta t d^2 \left(\frac{\Delta\rho_p}{\Delta\phi}\right)^2 \quad \text{(summation)} \tag{3b}$$

$$\Delta\rho_T = \sqrt{\Delta\rho^2 + (v\Delta t)^2} \quad \text{(no summation)} \tag{4a}$$

$$= \sqrt{\Delta\rho^2 + \Delta\rho_p^2 + (v\Delta t)^2} \quad \text{(summation)} \tag{4b}$$

Many parameters present in Eqs. (2a), (2b), (3a), (3b), (4a), and (4b) have values that can be directly measured from intact eyes using anatomical, optical, and physiological methods. These include the facet lens diameter

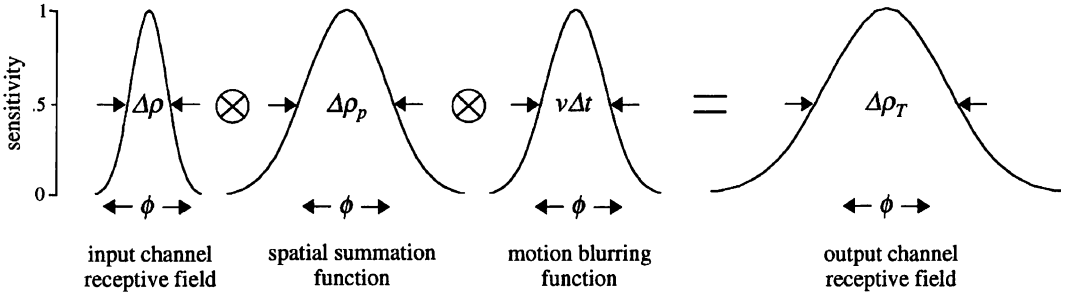

Fig. 1. Schematic of the basic summation model. A simple model of spatiotemporal summation. The receptive field of the output channel is determined by the receptive field of the input channel (the photoreceptor) and by the extent of spatial and temporal summation. The photoreceptor's receptive field is modeled as a Gaussian of half-width $\Delta\rho$ degrees. Greater temporal summation is modeled by increasing the integration time Δt (s). A longer integration time affects the spatial resolution of moving objects, which become spatially blurred by an amount $v\Delta t$ degrees, where v is the image velocity (deg s^{-1}). A motion blurring function can be modeled as a Gaussian of half-width $v\Delta t$ degrees (Snyder, 1977), which naturally only applies in the direction of motion. Greater spatial summation is modeled by widening the extent of coupling between neighboring ommatidia. The extent of coupling is modeled by a spatial summation function of angular half-width $\Delta\rho_p$; greater spatial summation is represented by a larger value of $\Delta\rho_p$. We can model the output receptive field as the convolutions of the input channel receptive field, the spatial summation function and the motion blurring function (circle-with-cross symbolizes convolution). The output channel receptive field is a Gaussian of half-width $\Delta\rho_T$ degrees [given by Eqs. (4a) and (4b)]. Adapted from Warrant, 1999.

(D), the rhabdom length (l) and diameter (d), the photoreceptor acceptance angle ($\Delta\rho$), the absorption coefficient of the rhabdom k, taken as 0.0067 μm^{-1}: (Bruno, Barnes, & Goldsmith, 1977), the quantum capture efficiency of the transduction process (κ, taken as 0.5; Lillywhite, 1977), the fraction of incident light transmitted by the optics of the eye (τ, taken as 0.9), and the specific dark variance (ω, taken as 1.3×10^{-6} equivalent photons $\mu m^{-3}\, s^{-1}$: Lillywhite, 1977; Lillywhite & Laughlin, 1979). Values and units of all parameters are given for the nocturnal halictid bee *M. genalis* and the honeybee *Apis mellifera* (provided as a diurnal comparison) in Table 1.

The integral term in Eqs. (2a) and (2b) describes the number of photons that will be absorbed in a photoreceptor of spectral sensitivity, $R(\lambda)$, viewing an illumination spectrum of quantal intensity, $I(\lambda)$, where λ is wavelength. That $R(\lambda)$ is in an exponent accounts for the important effect of self-screening (Warrant & Nilsson, 1998). The integral is calculated between two wavelength limits: $\lambda 1$ and $\lambda 2$, where $\lambda 1$ is set at 280 nm, the lowest wavelength likely to be seen by any animal, and $\lambda 2$ is the wavelength at which the spectral sensitivity $R(\lambda)$ falls to 1% of its maximum at the long wavelength end. In the Stavenga–Smits–Hoenders template $\lambda 2 = 1.231\ \lambda_{max}$, where λ_{max} is the absorbance peak wavelength of the visual pigment (Stavenga, Smits, & Hoenders, 1993). In our calculation $\lambda_{max} = 540$ nm, and thus $\lambda 2 = 665$ nm. $I(\lambda)$ was taken as the spectrum obtained from daylit green foliage (Warrant & Nilsson, 1998). This is a fair estimation for sunlit and moonlit foliage, but starlight is somewhat redder, and might further decrease the available photons. The terms before the integral simply determine the number of these photons that the optics of the eye allows to reach the photoreceptor. $R(\lambda)$ is calculated using the Stavenga–Smits–Hoenders rhodopsin template with peak spectral sensitivity at 540 nm.

The model described above has four important variables (Fig. 1): the light intensity ($I(\lambda)$), the angular velocity (v) of the image seen by the moving animal, the half-width ($\Delta\rho_p$) of the Gaussian function specifying the extent of spatial summation, and the integration time (Δt) which specifies the extent of temporal summation.

In this study, $\Delta\rho_p$ is used to predict the angular diameter of the dendritic fields of the first-order interneurons, or L-fibers, in the lamina. This diameter is an L-fiber's presumed spatial summation field, which assumes that the neuron's dendrites make synaptic contacts with the lamina cartridges that are visited. A larger value of $\Delta\rho_p$ is equivalent to a greater neural dendritic field area and a larger number of cartridges to which the L-fibers may connect. In other words, a larger value of $\Delta\rho_p$ corresponds to a greater extent of spatial summation. The angular area of spatial summation calculated by the model is circular: $\left(\left(\frac{\pi}{4}\right)\Delta\rho_p^2\right)$. The number of lamina cartridges, N_c, that are connected by this circular summation field is then simply given by

$$N_c = \frac{\pi\Delta\rho_p^2}{4\delta}, \tag{5}$$

where δ is the number of square degrees of visual space viewed by a single cartridge. δ depends on the angular packing of cartridges in the lamina, and this is accurately known for *M. genalis* (Fig. 2). As explained in Fig. 2, δ is calculated as 2.67 deg^2 in *M. genalis* and estimated as 4.8 deg^2 in *A. mellifera* (see also Table 1). It should be stressed that Eq. (5) is only an approximation—the model is based on Gaussians, and these result in circular summation fields. In reality the summation fields in angular space are either slightly elliptical (for example L-fibers L2 and L3) or very elliptical (for example L4) (see Section 4 and Fig. 8).

Table 1
Glossary of symbols with species-specific values

Symbol	Meaning	Units	Megalopta	Apis
Constants				
$\Delta\phi$	Interommatidial angle	Deg	1.4	1.9
$\Delta\rho$	Photoreceptor acceptance angle (half-width of photoreceptor's receptive field)	Deg	5.6	2.6
k	Absorption coefficient of the photoreceptor	μm^{-1}	0.0067	0.0067
κ	Quantum efficiency of transduction	—	0.5	0.5
ω	Specific dark variance	Equivalent photons $\mu m^{-3}\, s^{-1}$	1.3×10^{-6}	1.3×10^{-6}
d	Photoreceptor diameter	μm	8	2
l	Photoreceptor length	μm	350	320
δ	Angular area viewed by one cartridge	Deg^2	2.67	4.8
D	Diameter of the facet lens	μm	36	20
τ	Transmission of the eye's optics	—	0.9	0.9
m	Mean contrast of the scene	—	0.4	0.4
Variables				
N	Photons captured by a photoreceptor in one integration time	photons		
$I(\lambda)$	Quantal intensity of a green foliage spectrum	Photons $\mu m^{-2}\, s^{-1}\, sr^{-1}\, nm^{-1}$		
$R(\lambda)$	Spectral sensitivity of a green photoreceptor ($\lambda_{max} = 540$ nm)	—		
λ	Wavelength	nm		
σ_D^2	Total dark variance	equivalent photons		
$\Delta\rho_p$	Half-width of spatial summation function	Deg		
$\Delta\rho_T$	Half-width of receptive field of output of visual channel	Deg		
v	Image velocity	$Deg\, s^{-1}$		
Δt	Integration time	s		
v_{max}	Maximum detectable spatial frequency	Cycles deg^{-1}		

Data for *M. genalis* and *A. mellifera* were taken from Warrant et al. (2004) and Greiner et al. (2004a). Values of k are from lobsters (Bruno et al., 1977). Values of D, l, $\Delta\phi$, and $\Delta\ \rho$ were taken from the frontal–ventral eye regions of both species. ω and κ are unknown for bees, so locust values were used (Lillywhite, 1977; Laughlin & Lillywhite, 1982). δ was calculated as 2.67 deg^2 for *M. genalis* from Fig. 2, and was estimated for *A. mellifera* assuming that the packing of ommatidia (and cartridges) is similar in the oval eyes of both species, but is simply more dilute in *A. mellifera*. For *A. mellifera*, with an average $\Delta\phi$ of 1.9°, δ was estimated at $2.67(1.9/1.4)^2 = 4.8\ deg^2$, where $\Delta\phi = 1.4°$ in *M. genalis*. In calculations of optimal v_{max} as a function of light intensity, the lowest values of Δt corresponded to light-adapted photoreceptor values (20 ms in *M. genalis* and 10 ms in *Apis*). In calculations of optimal v_{max} as a function of angular velocity at the dimmest behavioral light levels, the lowest values of Δt corresponded to dark-adapted photoreceptor values (32 ms in *M. genalis* and 18 ms in *Apis*). Photoreceptor values of Δt were taken from Warrant et al. (2004).

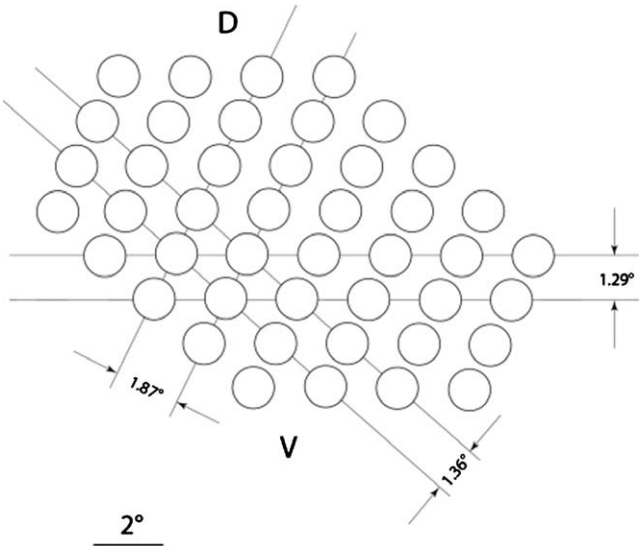

Fig. 2. Measured angles between facets of the frontal bee eye. The packing of ommatidia (symbolized by circles), and thus lamina cartridges, in angular visual space. Packing is shown for the frontal-ventral eye region of *M. genalis* (latitude −20°, longitude 20°: see Warrant et al., 2004). Horizontal rows of ommatidia are the most tightly packed, being only 1.29 deg apart, a direct result of the elongated oval shape of the eye. An average interommatidial angle of 1.4° can be derived from the angular packing of ommatidia in the three row directions. Data from Warrant, Kelber, Wcislo, & Gislén (in preparation). The average number of square degrees of visual space δ viewed by a single lamina cartridge within this packing lattice was calculated to be 2.67 deg^2. D, dorsal; V, ventral.

A longer response time in dim light (Δt) increases the signal-to-noise ratio and improves contrast discrimination by suppressing photon noise at temporal frequencies that are too high to be resolved reliably (Van Hateren, 1993). For ease of modeling, Snyder, 1977 represented this low pass filtering by a finite visual integration time Δt. Like the shutter time of a camera, a longer visual integration time improves the reliability of images in dim light Eqs. (2a) and (2b), but only at the expense of temporal resolution (Warrant, 1999). Temporal summation was simulated in *M. genalis* and *A. mellifera* by allowing Δt to exceed values measured in the dark-adapted photoreceptors.

The effects of integration time and image motion on spatial resolution can be modeled by a "motion blurring function" (Srinivasan & Bernard, 1975; Snyder, 1977), again assumed Gaussian for simplicity (Fig. 1). If an object moves with an angular velocity v deg s^{-1}, then during one integration time (Δt) its image is displaced an angular distance of $v\Delta t$ degrees across the retina. This additional spatial uncertainty associated with motion can be modeled with a motion blurring function of half-width $v\Delta t$. A fast image velocity or a long integration time (due to temporal summation) result in a loss of spatial resolution by widening the motion blurring function.

The image velocities (v deg s^{-1}) experienced by flying nocturnal bees while viewing landmarks at night were estimated from the recorded orientation flight shown in Warrant et al. (2004). Actual image velocities are angular velocities across the retina, which are generated both by motion in the environment and self-motion. Estimation of self-motion is especially relevant to flying animals, and comprises translational and rotational components. Importantly, translation generates angular velocities that depend on object distance, while rotation does not. Since object distance varies enormously for flying bees—ranging between celestial objects at optical infinity, to nests less than a centimeter away—we considered only the rotational movements of the bee. For *M. genalis*, the measured image velocities were highly variable, ranging from 75 to 450 deg s^{-1} with an average of 240 deg s^{-1}. For the calculations described below (with *M. genalis* and *A. mellifera*), image velocities ranging from 50 to 500 deg s^{-1} were chosen.

2.2. Calculation procedure

At each light intensity and for a given image velocity (usually 240 deg s^{-1}: see above), a physiologically plausible range of values for $\Delta\rho_p$ and Δt were used to calculate v_{max}. The combination of $\Delta\rho_p$ and Δt that resulted in the largest v_{max} at each intensity was then considered the optimum extent of spatial and temporal summation. Identical calculations were performed for *M. genalis* and *A. mellifera* (using the appropriate values of parameters given in Table 1).

The values of $\Delta\rho_p$ derived from the optimization were then used to calculate the number of lamina cartridges [N_c: Eq. (5)] predicted to be involved in spatial summation. These values of N_c were then compared to known lamina cell morphologies to see whether the model also predicts the observed branching patterns of L-fibers (Greiner et al., 2004b, 2005).

3. Results

Model results show that summation, based on an optimal combination of spatial and temporal pooling, improves v_{max} at dim light intensities, thus extending the range of reliable vision. Fig. 3 shows the finest spatial frequency visible to *M. genalis* (A), and *A. mellifera* (D), as calculated by Eqs. (2a) and (2b), over a range of natural light intensities. In this case, image velocity was held fixed at 240 deg s^{-1} (measured from *M. genalis* during a nocturnal foraging flight: (Warrant et al., 2004). When bees sum photons optimally in space and time (*solid lines*) vision is extended to much lower light intensities (non-zero v_{max}) compared to when summation is absent (*dashed lines*). In *A. mellifera*, for example, at 1.5 log units of intensity (photons μm^2 s^{-1} sr^{-1}) v_{max} improves from 0.0361 cycles deg^{-1} without summation to 0.0853 cycles deg^{-1} with summation. Although the European honeybee is not usually active at these light intensities, some Africanized races of *A. mellifera* continue to forage on moonlit nights (Fletcher, 1978). In *M. genalis*, a dramatic improvement of visual performance by neural summation is present across the entire range of light intensities when these bees are active (Fig. 3A). For instance, at 0.0 log units of intensity, v_{max} improves from 0.030 to 0.073 cycles deg^{-1} during summation. Overall, nocturnal bees can see in dimmer light than honeybees, but honeybees can see higher spatial frequencies in bright light.

These improvements resulted from both temporal and spatial summation. The optimal values of integration time, Δt, representing temporal summation, are shown in Fig. 3 for *M. genalis* (B), and *A. mellifera* (E). At lower light intensities longer integration times are predicted to be optimal, while at higher light intensities integration times approached values measured from light-adapted photoreceptors. In both species integration times are predicted to be longer at the dimmer end of their activity windows. However, at the example intensity of 0.0 log units for *M. genalis*, Δt is only 20 ms with summation, while it was 36 ms without summation. This is due to the high angular velocity used in this calculation, and is an example of the tradeoffs that can be made between spatial and temporal summation. In this case, the need to maximize temporal resolution results in a shorter

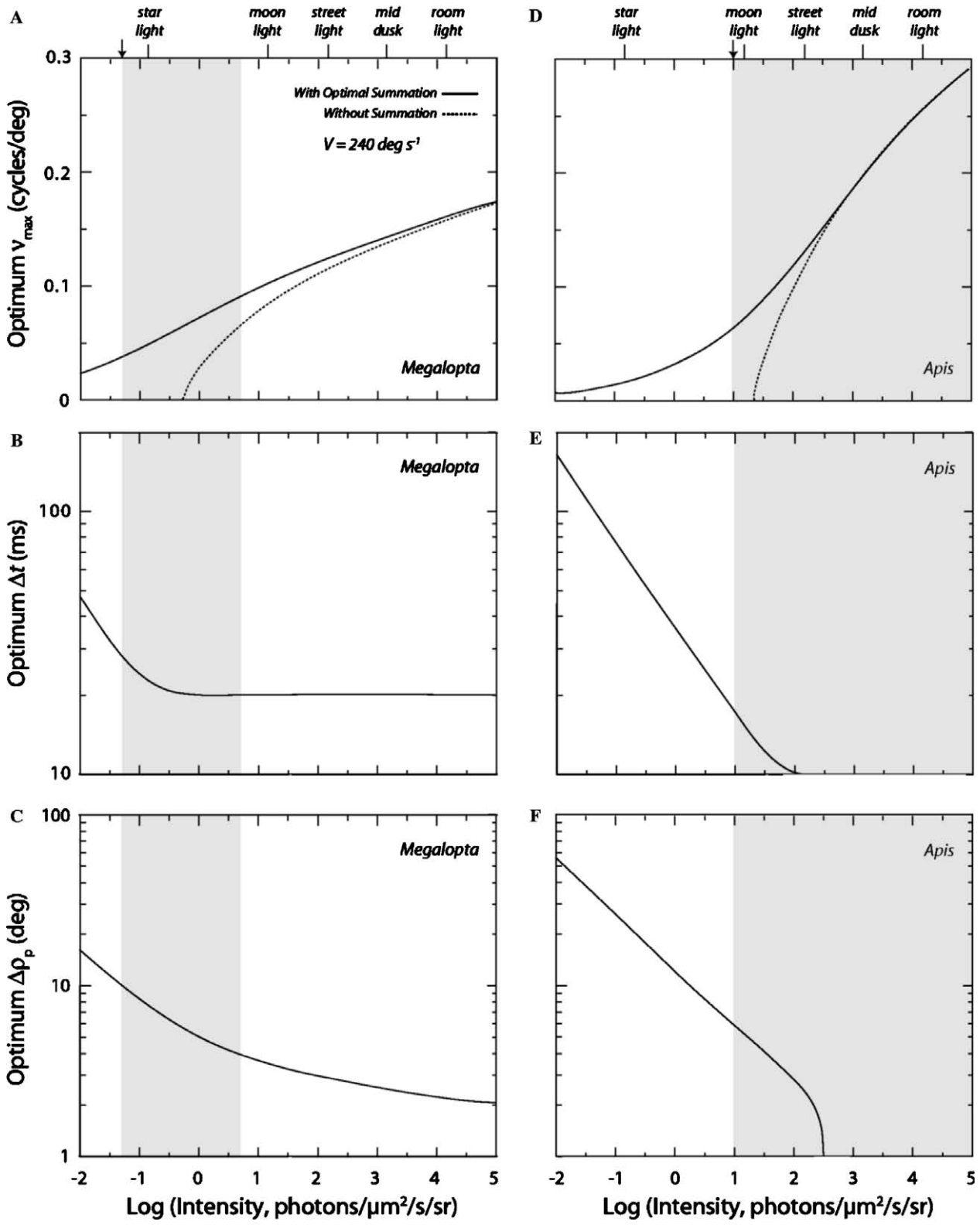

Fig. 3. Optimal summation varying with light intensity. Spatial and temporal summation modeled at different light intensities in the nocturnal halictid bee *M. genalis* (A–C) and the honeybee *A. mellifera* (D–F) for an image velocity of 240 deg s^{-1}. Light intensities are given for 540 nm, the bee's peak spectral sensitivity, and given in $\mu m^2\ s^{-1}\ sr^{-1}$, a unit convenient for nocturnal insect vision. Grey areas denote the light intensity window within which each species is normally active. Arrowheads denote the lowest light intensities experienced by *M. genalis* and *A. mellifera* (−1.3 and 1.0 log units of intensity, photons, respectively). (A and D) The finest spatial frequency visible to flying bees (as measured by the maximum detectable spatial frequency, v_{max}), with (solid lines), and without (dashed lines) optimal summation. (B and E) The integration times, Δt, necessary for allowing the visible frequencies plotted in (A and D). (C and F) The summation function half-widths, $\Delta\rho_p$, necessary for allowing the visible frequencies plotted in (A and D).

integration time and less temporal summation—visual reliability is instead improved by greater spatial summation (see below). The same is true for *A. mellifera* at the example intensity of 1.5 log units; here Δt is 12 ms with summation and 18 ms without.

The optimal values of the summation function half-width, $\Delta\rho_p$, representing spatial summation, are shown for *M. genalis* (Fig. 3C), and *A. mellifera* (Fig. 3F). At lower light intensities, greater half-widths were necessary, indicating that optimal visual performance largely depends on the spatial summation of signals from neighboring ommatidia. Here, at our example intensities, $\Delta\rho_p$ is predicted to be 5.1 deg in *M. genalis* and 3.5 deg in *A. mellifera*. In both species, spatial summation noticeably increases at the dimmer end of their activity windows. At higher intensities, spatial summation is predicted to be absent. However, we can also see that for *A. mellifera* above 2.0 log units of intensity, while some summation is still present, it is entirely spatial. Again this results from the relatively high image velocity used in this calculation, and at higher intensities spatial summation is favored to maintain temporal resolution.

To illustrate the independent effects of spatial and temporal summation, we repeated the intensity simulation for *M. genalis* at its natural light intensities, but allowed only temporal or spatial summation, (Fig. 4). Again we used an image velocity of 240 deg s^{-1}, but at this velocity optimal summation is almost exclusively spatial (Fig. 3B), so the comparison is between optimal summation and temporal summation only. Temporal summation only is inferior to full summation, as measured by v_{max} (Fig. 4A). Not only is the highest detectable frequency lower at all of *M. genalis*'s active light levels, the difference increases as light wanes. The temporal summation required to produce these detectable frequencies is small if spatial summation is allowed, but large otherwise (Fig. 4B). As light level drops, optimal pooling involves very little spatial summation. If this is not allowed, temporal summation rises exponentially in decreasing light to optimize vision. In both cases the minimal value of Δt approaches the integration time of the photoreceptor. The corresponding $\Delta\rho_p$ confirms that optimal summation at this velocity relies on spatial summation, and vision degrades if it is optimized only with temporal summation (Fig. 4C).

In the next case, we optimized v_{max} over a range of angular image velocities, this time holding the light intensity fixed (Fig. 5). Here, light level was fixed at the lowest intensities experienced by *M. genalis* and *A. mellifera* (−1.3 and 1.0 log units of intensity: see arrowheads in Fig. 3). The range of velocities was chosen to reflect plausible values experienced by flying bees during landmark orientation flights. The finest spatial frequency visible to flying bees decreases with increasing image velocity, although at all velocities v_{max} is higher in *A. mellifera* than in *M. genalis* (Fig. 5A). The extent of spatial and temporal summation is predicted to be greater for *M. genalis* than for *A. mellifera*, but for both, as image velocity increases, Δt decreases

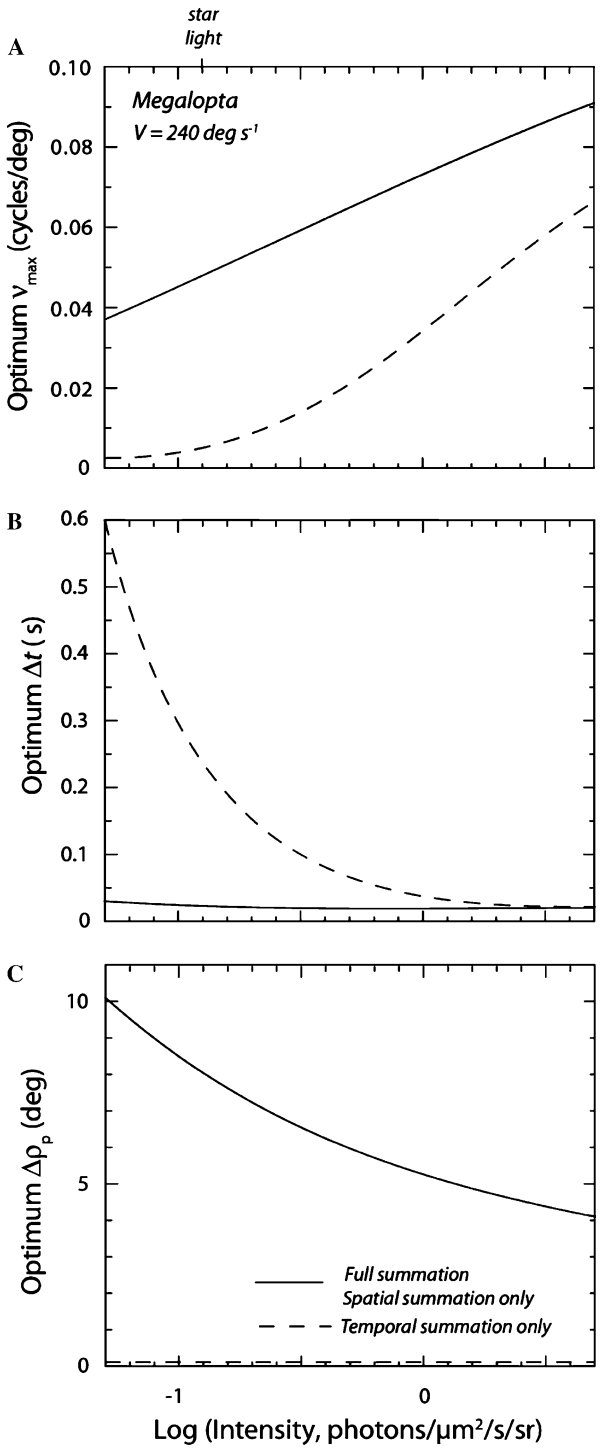

Fig. 4. Temporal and spatial summation only against intensity. Spatial and temporal summation modeled independently in *M. genalis* over its active light range, for an image velocity of 240 deg s^{-1}. Notably, at these light levels and velocity, the optimal summation is spatial summation only, or very nearly, so full and spatial summation are the same on the plots. This would be different for other intensities and image velocities. (A) The finest spatial frequency visible to flying bees (as measured by the maximum detectable spatial frequency, v_{max}), with spatial summation (solid lines), or temporal summation (dashed lines). (B) The integration times, Δt, that allow the visible frequencies plotted in (A). The dashed line optimized with temporal pooling only. (C) The summation function half-widths, $\Delta\rho_p$, that allow the visible frequencies plotted in (A). The dashed line optimized with no spatial summation.

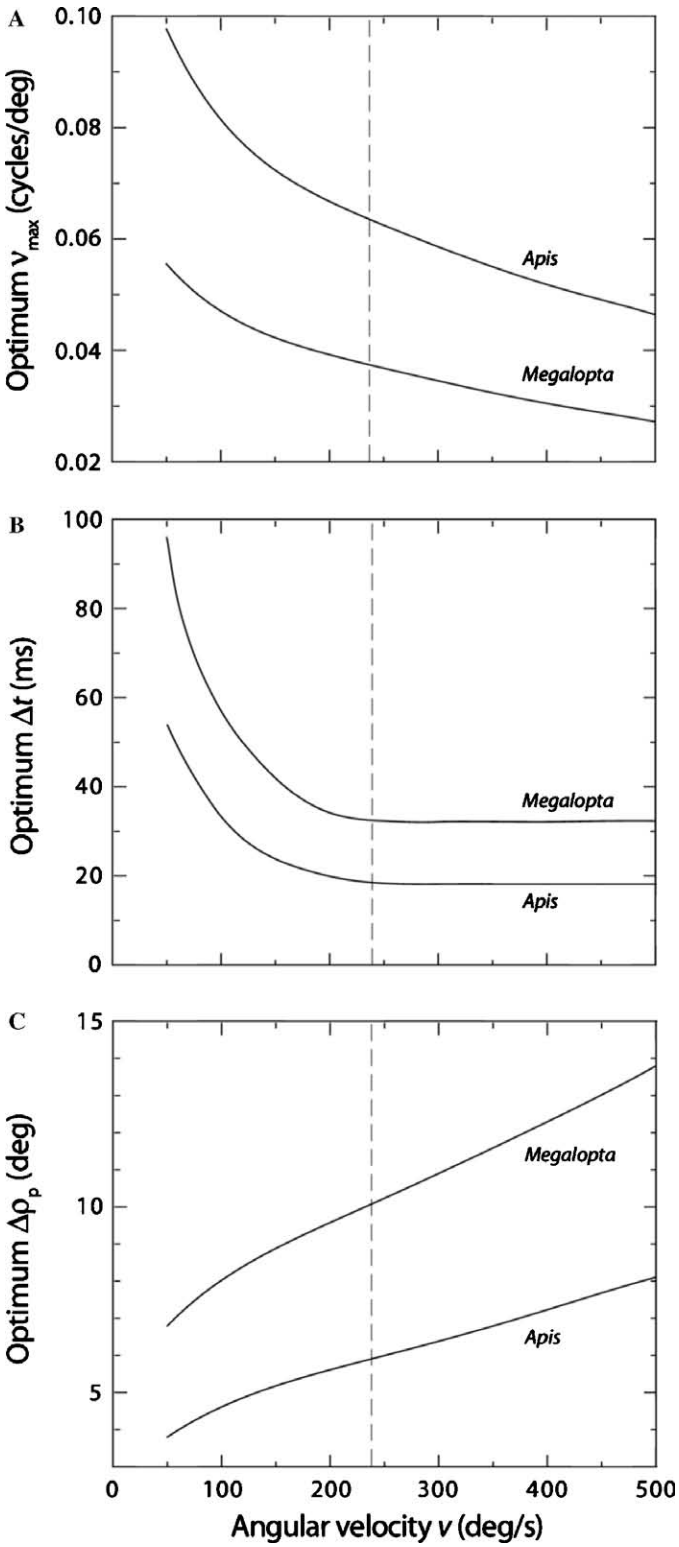

Fig. 5. Optimal summation varying with angular velocity. Spatial and temporal summation modeled for different image angular velocities, v, at the lowest light intensities experienced by *M. genalis* and *A. mellifera* (−1.3 and 1.0 log units of intensity, photons μm^2 s^{-1} sr^{-1}, respectively). *Vertical dashed lines* indicate $v = 240$ deg s^{-1}, the value chosen for Fig. 3. (A) The finest spatial frequency visible to flying bees [as measured by the maximum detectable spatial frequency, v_{max}: Eqs. (2a) and (2b)]. (B) The integration times, Δt, that were necessary for allowing the finest visible spatial frequencies plotted in (A). (C) The summation function half-widths, $\Delta\rho_p$, that were necessary for allowing the finest visible spatial frequencies plotted in (A).

(Fig. 5B) while $\Delta\rho_p$ increases (Fig. 5C). High image velocity tips the balance between spatial and temporal summation in favor of spatial summation, to maintain reasonable temporal resolution.

Optimal spatial summation was then translated to N_c, the predicted number of lamina cartridges summed (Fig. 6). As before, we calculated this as a function of image velocity (Fig. 6A), and light intensity (Fig. 6B). In the first case, N_c was calculated over a range of image angular velocities while light intensity was held constant. Intensity was set to −1.3 log units for *M. genalis*, and 1.0 log units for *A. mellifera*—the lowest intensities experienced by each during flight. Because the extent of spatial summation is predicted

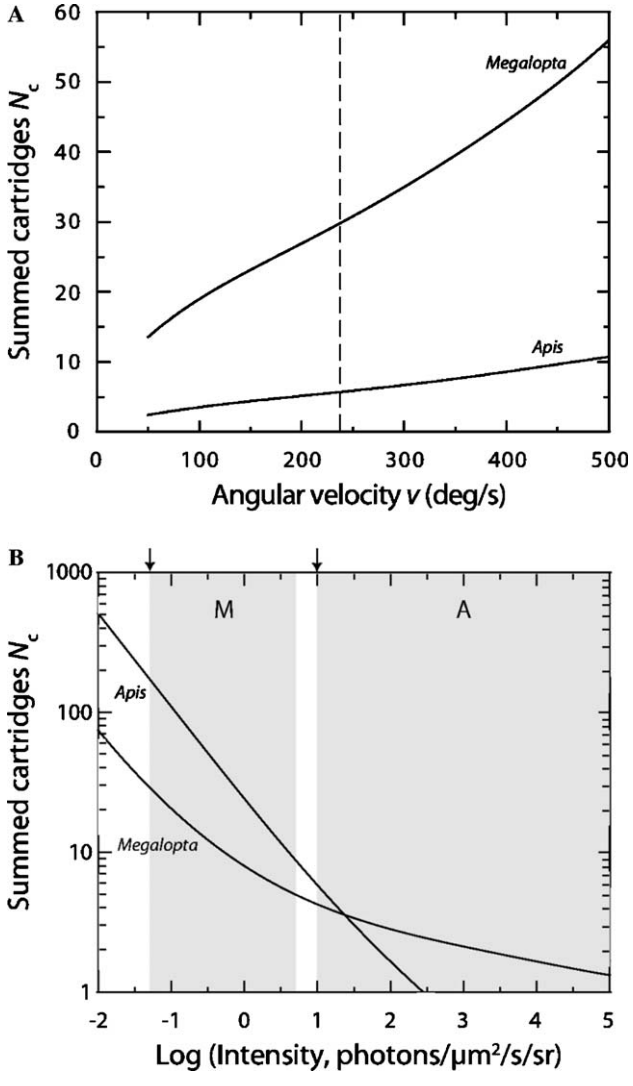

Fig. 6. Optimal number of summed facets as velocity and brightness vary. The number of lamina cartridges N_c [Eq. (5)] in *M. genalis* and *A. mellifera* that are predicted to be involved in spatial summation as a function of image angular velocity (A) and light intensity (B). (A) N_c as a function of image angular velocity, v, at the lowest light intensities experienced by *M. genalis* and *A. mellifera* (−1.3 and 1.0 log units of intensity, photons μm^2 s^{-1} sr^{-1}: see arrowheads in B). Dashed line indicates $v = 240$ deg s^{-1}, the value chosen for Fig. 3. (B) N_c as a function of light intensity for an image velocity $v = 240$ deg s^{-1}. Grey areas denote the light intensity window within which each species is normally active (M, *M. genalis*; A, *A. mellifera*).

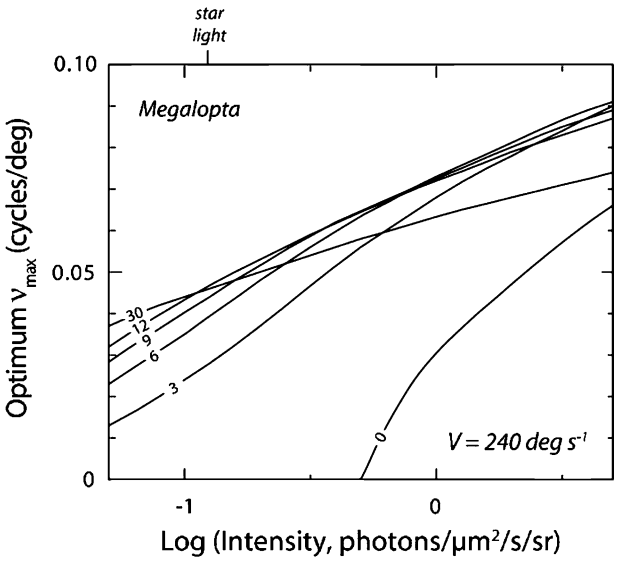

Fig. 7. Sensitivity of the model to cartridge pooling. The finest spatial frequency visible to flying *M. genalis* [as measured by the maximum detectable spatial frequency, v_{max}: Eqs. (2a) and (2b)] as a function of light intensity for various extents of spatial summation: for no summation, and for 3, 6, 9, 12, and 30 summing cartridges. All calculations were made at a single image velocity, $v = 240$ deg s^{-1}, and for the light intensity range normally experienced by *M. genalis* (−1.3 to 0.7 log units, photons μm^2 s^{-1} sr^{-1}).

to increase with image velocity (Fig. 5B), the number of cartridges involved in spatial summation is also predicted to increase. At any given image velocity the number of cartridges is predicted to be greater in *M. genalis* than in *A. mellifera*: at $v = 240$ deg s^{-1}, 30 cartridges are predicted to be involved in summation in *M. genalis* compared to 6 for *A. mellifera*. Likewise in the second case, N_c was calculated over a range of light intensities. Here velocity was held constant at 240 deg s^{-1}. Because the extent of spatial summation is predicted to increase with decreasing light intensity (Figs. 3C and 3F), the number of cartridges involved in spatial summation is also predicted to increase. Here, the predicted number of summed cartridges is lower for *M. genalis* in dim light than for *A. mellifera* due to the enhanced optical sensitivity of their eyes.

N_c is quite high at the lowest intensities, so to test the model's sensitivity to cartridge number, we held cartridges summed constant and calculated the finest spatial frequencies, v_{max}, visible at constant velocity during *M. genalis*'s active period of light intensities (Fig. 7). Throughout most of this light intensity range, spatial summation from between 9 and 12 cartridges is predicted to be better overall than summation from 30 cartridges (only predicted to be optimal for the lowest light intensities, less than −1.0 log unit of intensity).

4. Discussion

Summation appears to improve vision over a wider range of intensities in *M. genalis* than in *A. mellifera*. The honeybee benefited from summation (as measured by improvement in v_{max}) only at light levels equivalent to mid dusk to moonlight. Even though the European honeybee does not forage at these light intensities, the Africanized honeybee *Apis mellifera adansonii* is an active nocturnal forager (Fletcher, 1978) that would clearly benefit from the predicted summation (Warrant et al., 1996). The nocturnal bee benefits from summation at every intensity at which it is known to fly. At the dimmest light intensities of their activity periods, both species are predicted to benefit from summation, but whether this is spatial or temporal summation depends on the image angular velocity.

Temporal summation can be implemented in a single visual channel, but spatial summation requires pooling of the otherwise discrete lamina cartridges that correspond to insect ommatidia. The number of cartridges required to implement the optimal spatial summation grew with higher velocities, but particularly so with lower intensities.

Visual summation offers clear theoretical benefits, but to realize these, the strategies must be physically implemented by the nervous system. Spatial summation is likely to take place in the lamina, where the first visual synapses, between photoreceptor cell axons and first-order interneurons are formed. To mediate spatial summation these neurons need to project dendritic branches to several neighboring cartridges. The optimal dendritic field suggested by the model (N_c) for most of the light intensities experienced by *M. genalis* during foraging involves coupling of around 12 cartridges (Fig. 7). This closely matches the number of cartridges inside the dendritic field of L-fibers L2 and L3 (Fig. 8). Lateral branches of L2 and L3 extend over a total number of 13 and 12 cartridges, respectively, and the dendritic field of L4 extends even further, to a total of 18 cartridges (Fig. 8, Greiner et al., 2005). Again it should be stressed that calculated values of N_c are approximate. The model assumes symmetric summation, whereas the L-fibers clearly indicate elliptical summation fields.

For *A. mellifera*, N_c was under 10 for all image velocities and light intensities within their normal active range ($N_c = 6$ for $v = 240$ deg s^{-1}; $I = 1.0$ log units of intensity). This also agrees closely with neural anatomy where L2 and L4 target 8 and 6 neighboring neurons respectively, for a total of 9 and 7 potentially summed cartridges (Greiner et al., 2005).

The fact that some honeybee L-fibers branch to neighboring cartridges, despite the honeybee being a predominantly diurnal animal, is an interesting point. The L-fibers of other strictly diurnal insects, such as dragonflies (Meinertzhagen & Arnett-Kibel, 1982), butterflies (Strausfeld & Blest, 1970), and houseflies (Boschek, 1971; Strausfeld, 1971), do not branch to neighboring cartridges. The presence of branching L-fibers in ancestral honeybees may have allowed the evolution of nocturnal activity in the Africanized race of *A. mellifera*, as well as in the giant Asian honeybee *Apis dorsata* (Dyer, 1985). In the warm competitive habitats where these bees forage, spatial summation may have allowed them to exploit a nocturnal

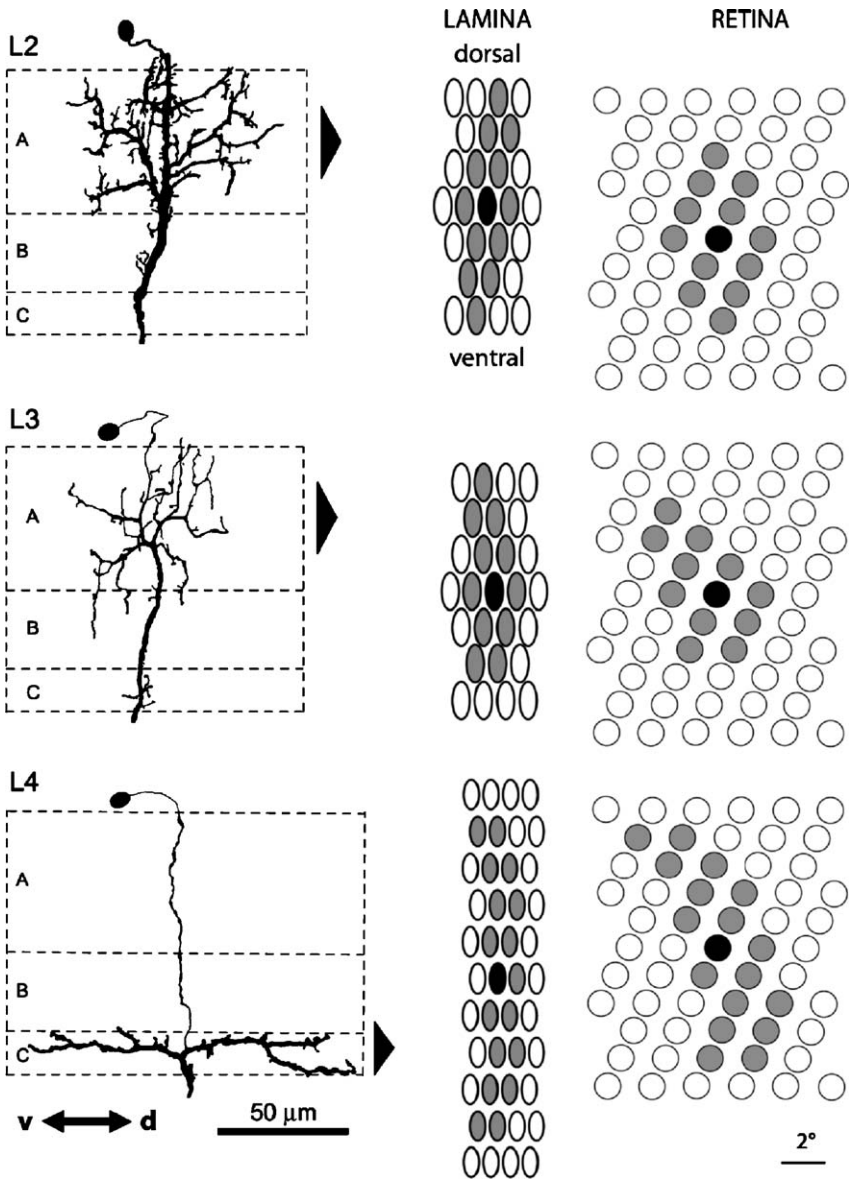

Fig. 8. Anatomy of some *M. genalis* lamina cells. The dendritic fields of laterally spreading first-order interneurons (L-fibers) in the lamina of *M. genalis* suggest their potential role in spatial summation. (Left column) The lateral branching pattern within the three lamina layers A, B, and C classifies the L-fiber types L2, L3, and L4. v, ventral; d, dorsal. (Center column) The schematic cross section of the dendritic fields in linear (anatomical) space (grey circles) is shown in layer A for L2 and L3 and in layer C for L4, where L2, L3, and L4 contact 12, 11, and 17 cartridges respectively. The black circles symbolize each neuron's parental cartridge. (Right column) The dendritic fields superimposed onto the angular packing matrix of the ommatidia (Fig. 2), indicating their angular visual fields. Scale bar, 2°.

niche. European honeybees, possibly due to lower competition, simply remained diurnal.

4.1. A simulation of Megalopta spatial summation

To simulate the possible visual benefits of these cells, we began with two photographs from a bee habitat (Fig. 9, top row). One is a view of a nest entrance photographed from a distance of five centimeters, the other a view of the overhead canopy, from ground level. Both are likely to represent crucial navigational cues for *M. genalis*. We simulated spatial summation with hexagonal kernels for visual convolution. The shape of these arrays reflects the anatomy of the neurons, and we assume they completely pool the visual signals of all cartridges they touch. For summation we chose one highly symmetrical cell (Fig. 9, insets: left, middle) and one highly vertical cell (Fig. 9, insets: left, bottom). The vertical cell is based on L4 from Fig. 8 and the symmetrical cell, although not shown in Fig. 8, is based on the anatomy of L-fibers found in *M. genalis* (for example L1-b in (Greiner et al., 2005).

To determine the light gathered in each ommatidium, we began with the angular acceptance function, an empirically determined measure of how well off-axis light

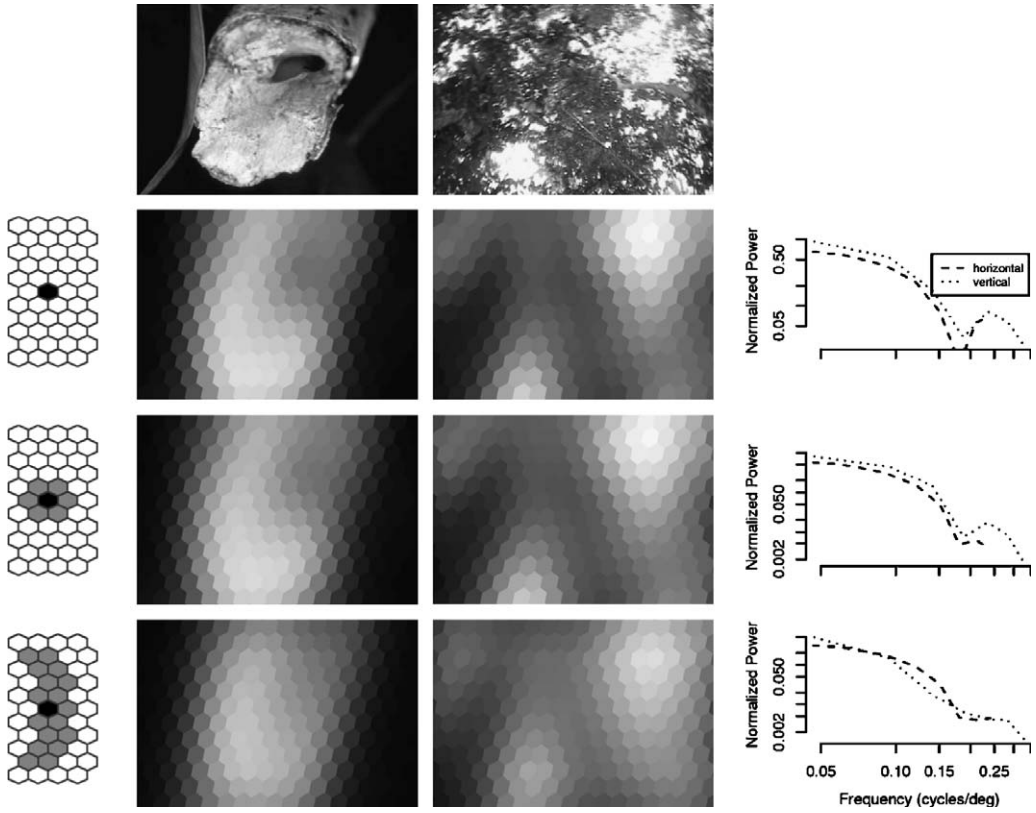

Fig. 9. Simulated summation on *M. genalis* vision. Two images from *M. genalis*'s habitat on Barro Colorado Island (upper row), a nest and the canopy overhead, were subjected to spatial summation (bottom two rows) suggested by neural anatomy (insets: left). The unpooled view (second row) is already substantially blurred by the optics. Acuity loss that results from summation largely overlaps this blur, and little additional detail is lost. The modulation transfer functions (insets: right) were computed for both the horizontal (dashed lines) and vertical (dotted lines) directions of the bee's visual field.

stimulates a single photoreceptor. We measured light stimulation between ±7 degrees (Warrant et al., 2004), and fit the resulting curve with a sum of two Gaussian functions. The receptors are packed in visual space as an irregular hexagonal array (Fig. 2) and each photograph subtends approximately 30×20 visual degrees, which accommodated 300 receptors. These angles do not map perfectly onto a plane—nor should they since the bee eye is curved—so the largest inter-row angle was expanded to produce the images. Visual space is properly represented on the surface of a sphere, but for small visual angles a flat map is acceptable. The largest inter-ommatidial angle increased by 10%, and the result is purely a matter of display. The summation was implemented by a convolution that was coded to work with hexagonal arrays. The new response of each facet was the normalized sum of all the facets touched by a superimposed kernel. This is what the cellular anatomy suggests may actually happen—a facet's response may pool with several neighboring facets.

Additionally, the modulation transfer functions (MTFs) of the processed visual image were computed with discrete Fourier transforms of point spread functions. These were applied in the horizontal and vertical directions, with and without summation. This shows differences induced by the irregularity of the facet packing, and the asymmetry of the summation, by showing the contrast present in the image as a function of spatial frequency.

The simulated bee view illustrates that a nocturnal bee receives a compromised image (Fig. 9, second row). This is only partly due to the inherent poor spatial resolution of compound eyes, but is made much worse by the broad angular acceptance of each ommatidium. Considerable blurring occurred even without neural summation. As a result, however, the summation does surprisingly little additional damage to the image. What these figures do not show is the substantial noise reduction that summation implements. And while much detail is lost with these transformations, basic light patterns can still be recognized, both at the nest entrance and in the overhead canopy. The MTFs show that without summation some contrast remains at frequencies up to about 0.3 cycles deg^{-1}, and the vertical resolution is better than the horizontal (Fig. 9, insets: right, top). If symmetrical summation is applied, contrast disappears at lower spatial frequencies, about 0.20–0.25 cycles deg^{-1}, but vertical acuity remains higher (Fig. 9, insets: right, middle). Finally, the highly vertical summation reduced vertical contrast in the middle frequency ranges, between 0.07–0.17 cycles deg^{-1}, to below that of horizontal contrast (Fig. 9, insets: right, bottom).

In the dark, bee vision is degraded immediately by the initial angular acceptance function. It is wide in dark-adapted photoreceptors as a first means of improving photon catch (Warrant et al., 2004). Spatial summation largely overlaps with this acceptance function, however, and, as shown in Fig. 9, visibly does little to the image. In *M. genalis*, the acceptance angle is approximately four times the interommatidial angle (Table 1) and because of this large visual overlap, spatial summation should extend to at least those cartridges that are within two interommatidial angles of the central ommatidium. To do so would increase photon capture with no further loss in spatial resolution. This is corroborated by the summation scheme suggested by Fig. 8.

The dendritic fields of the L-fibers (and their suggested summation strategies) are also notable as some are symmetrical and others largely vertical. We have simulated the visual image resulting from the most vertical form of summation, as suggested by the L4 neuron, and found that the MTF notably loses contrast in the vertical direction (Fig. 9, insets: right, bottom): the bee's eyes are fundamentally more sensitive in this direction without summation (Fig. 9, insets: right, upper).

One possible explanation for this asymmetry is that the bee moves asymmetrically, in a primarily horizontal direction. In the frontal eye region, motion from forward translation is small and radially symmetrical, but bees rotate quickly in the horizontal plane, which generates fast horizontal motion and no vertical motion. Vertically pooling, then, might seem to run counter to the general prediction that greater angular velocities favor spatial pooling. However, this is not two cells viewing different velocities, it is a single cell with different components of velocity in angular space. Therefore, vertical pooling could offer the advantages of summation without sacrificing spatial resolution, at least not in the direction of interest. Along these same lines, it may be that in the visual environment of the rain forest, which is dominated by vertical trunks, vertical acuity captures less information than horizontal. In other words, vertical acuity may be more redundant than horizontal.

At night, a visually guided animal must cope with photon noise if it is to see at all. Large angular acceptance angles and spatial summation both reduce photon noise at the cost of spatial acuity, but they do so in different ways. If the nocturnal bee eye is already compromised with one form of noise reduction, it suffers little by implementing the other.

But the rain forest is a highly complex visual environment, and it is a wonder that an animal might navigate even with high visual acuity. *M. genalis* must leave its nest, find flowers which are not visible from the nest, and return to a cluttered area and relocate the nest entrance. In the evening, it must do this with special precision, as the light fades quickly. Bees are already subjected to poor spatial acuity by virtue of compound optics; how can *M. genalis* cope with further loss of acuity and still perform these tasks? This speaks to the fundamental question of how much resolution is required to navigate in the forest, which is unknown.

One possibility is that low pass filtering may improve a bee's ability to navigate. Consider the overhead view of the canopy, in which holes are randomly spaced and bright. These holes might serve as ideal guideposts, each position in the forest marked by a signature light pattern even at night. High acuity views of the canopy include leaves and small branches that change over short time scales and add nothing useful to location information. For a bee to navigate by these patterns, as shown for ants (Hölldobler, 1980), low spatial acuity might be preferable.

Finally, this model is based on data from one species, (*Megalopta genalis*), from one location, Barro Colorado Island (BCI), Panama. It implicitly assumes *M. genalis* is representative of *Megalopta*, and that BCI is representative of *Megalopta*'s habitat. Whether the first assumption is true is unsure, but the second assumption is certainly false. BCI's canopy is more open than that of mature, intact rain forests, yet more closed than that of dry forests where *Megalopta* also occur. To this end, we can use the results of our model to make predictions about the degree of summation we expect to find in different species, under different light environments, or populations of the same species in different light environments. For example, we can predict that other nocturnal bees and wasps living in much more open habitat, can either extend their active period further into the night, or rely less heavily on neural summation. In the latter case their neural anatomy should reflect such a difference. On the other hand, even *M. genalis* is known from much denser, more mature forests, and unless these sub-populations have differences in their neural anatomy and ability to implement neural summation (which is rather unlikely), we expect that they will be limited to a shorter time window for foraging. Such a limitation due to light intensity has also been shown in a smaller, closely related species, *Megalopta equadoria* and other crepuscular bees, whose activity periods are mainly restricted to higher intensities (Kelber et al., 2006).

Our results show that neural summation is extremely useful in insects active in dim light, turning a diurnal apposition eye into an acceptable nocturnal eye. With optimal spatiotemporal summation, vision can be extended into significantly dimmer light intensities and such an obvious beneficial effect can be expected to be widely used in the eyes of nocturnal animals.

Acknowledgments

We thank Melissa Coates for careful reading and valuable critique of the manuscript. E.J.W. is grateful for the ongoing support of the Swedish Research Council.

References

Arneson, L., & Wcislo, W. (2003). Dominant–subordinate relationships in a facultatively social nocturnal bee, *Megalopta genalis* (Hymenoptera: Halictidae). *Journal of Kansas the Entomological Society, 76*, 183–193.

Boschek, C. B. (1971). On the fine structure of the peripheral retina and lamina ganglionaris of the fly, *Musca domestica*. *Zeitschrift fur Zellforschung und Mikroskopische Anatomie, 118*, 369–409.

Bruno, M. S., Barnes, S. N., & Goldsmith, T. H. (1977). The visual pigment and visual cycle of the lobster *Homarus*. *Journal of Comparative Physiology, 120*, 123–142.

De Vries, H. (1943). The quantum character of light and its bearing upon threshold of vision, the differential sensitivity and visual acuity of the eye. *Physica, 10*, 553–564.

Dyer, F. C. (1985). Nocturnal orientation by the Asian honey bee, *Apis dorsata*. *Animal Behaviour, 33*, 769–774.

Fletcher, D. J. C. (1978). The African bee, *Apis mellifera adansonii*, in Africa. *Annual Review of Entomology, 23*, 151–171.

Greiner, B., Ribi, W., & Warrant, E. (2004a). Retinal and optical adaptations for nocturnal vision in the halictid bee *Megalopta genalis*. *Cell and Tissue Research, 316*(3), 377–390.

Greiner, B., Ribi, W. A., & Warrant, E. J. (2005). A neural network to improve dim-light vision. Dendritic fields of first-order interneurons in the nocturnal bee *Megalopta genalis*. *Cell and Tissue Research, 322*, 313–320.

Greiner, B., Ribi, W., Wcislo, W., & Warrant, E. (2004b). Neural organisation in the first optic ganglion of the nocturnal bee *Megalopta genalis*. *Cell and Tissue Research, 318*(2), 429–437.

Hess, R. F. (1990). Rod-mediated vision: Role of post-receptoral filters. In R. F. Hess, L. T. Sharpe, & K. Nordby (Eds.), *Night vision* (pp. 3–48). Cambridge: Cambridge University Press.

Hölldobler, B. (1980). Canopy orientation: A new kind of orientation in ants. *Science, 210*, 86–88.

Howard, J., & Snyder, A. (1983). Transduction as a limitation on compound eye function and design. *Proceedings of the Royal Society of London Series B, Biological Sciences, 217*, 287–307.

Jander, U., & Jander, R. (2002). Allometry and resolution of bee eyes (Apoidea). *Arthropod Structure and Development, 30*, 178–193.

Janzen, D. (1968). Notes on nesting and foraging behavior of *Megalopta* (Hymenoptera: Halictidae) in Costa Rica. *Journal of the Kansas Entomological Society, 41*, 342–350.

Kelber, A., Warrant, E. J., Pfaff, M., Wallén, R., Theobald, J. C., Wcislo, W. T., et al. (2006). Light intensity limits foraging activity in nocturnal and crepuscular bees. *Behavioral Ecology, 17*, 63–72.

Laughlin, S. (1981a). A simple coding procedure enhances a neuron's information capacity. *Zeitschrift fur Naturforschung C, 36*(9-10), 910–912.

Laughlin, S., & Lillywhite, P. (1982). Intrinsic noise in locust photoreceptors. *Journal of Physiology, 332*, 25–45.

Laughlin, S. B. (1981b). Neural principles in the peripheral visual systems of invertebrates. In H. Autrum (Ed.). *Handbook of sensory physiology* (Vol. VII/6B, pp. 133–280). Berlin: Springer.

Laughlin, S. B. (1990). Invertebrate vision at low luminances. In R. F. Hess, L. T. Sharpe, & K. Nordby (Eds.), *Night vision* (pp. 223–250). Cambridge: Cambridge University Press.

Lillywhite, P. (1977). Single photon signals and transduction in an insect eye. *Journal of Comparative Neurology, 122*, 189–200.

Lillywhite, P., & Laughlin, S. (1979). Transducer noise in a photoreceptor. *Nature, 277*(5697), 569–572.

Meinertzhagen, I. A., & Arnett-Kibel, C. (1982). The lamina monopolar cells in the optic lobe of the dragonfly *Sympetrum*. *Philosophical Transactions of the Royal Society of London Series B: Biological Sciences, 297*, 27–49.

Pelli, D. (1990). The quantum efficiency of vision. In Colin Blakemore (Ed.), *Vision: coding and efficiency* (pp. 3–24). Cambridge: Cambridge University Press.

Rose, A. (1942). The relative sensitivities of television pickup tubes, photographic film and the human eye. *Proceedings of the Institute Radio Engineers New York, 30*, 293–300.

Shapley, R., & Enroth-Cugell, C. (1984). Visual adaptation and retinal gain controls. In N. O. Osborne & G. J. Chader (Eds.), *Progress in retinal research* (pp. 263–346). London: Pergamon Press.

Sharpe, L. T. (1990). The light adaptation of the human rod visual system. In R. F. Hess, L. T. Sharpe, & K. Nordby (Eds.), *Night vision* (pp. 49–124). Cambridge: Cambridge University Press.

Snyder, A. (1977). Acuity of compound eyes: physical limitations and design. *Journal Comparative Physiology, 116*, 161–182.

Srinivasan, M. V., & Bernard, G. D. (1975). The effect of motion on visual acuity of the compound eye a theoretical analysis. *Vision Research, 15*, 515–526.

Stavenga, D., Smits, R., & Hoenders, B. (1993). Simple exponential functions describing the absorbance bands of visual pigment spectra. *Vision Research, 33*(8), 1011–1017.

Strausfeld, N. J. (1971). Organization of the insect visual system (light microscopy). 2. Projection of the fibres across first optic chiasma. *Zeitschrift fur Zellforschung und Mikroskopische Anatomie, 121*, 442–454.

Strausfeld, N. J., & Blest, A. D. (1970). Golgi studies on insects. Part I. The optic lobes of Lepidoptera. *Philosophical Transactions of the Royal Society of London Series B: Biological Sciences, 258*, 81–134.

Van Hateren, J. H. (1993). Three modes of spatiotemporal preprocessing by eyes. *Journal of Comparative Physiology A, 172*, 583–591.

Warrant, E. (1999). Seeing better at night: life style, eye design and the optimum strategy of spatial and temporal summation. *Vision Research, 39*(9), 1611–1630.

Warrant, E., Kelber, A., Gislén, A., Greiner, B., Ribi, W., & Wcislo, W. (2004). Nocturnal vision and landmark orientation in a tropical halictid bee. *Current Biology, 14*(15), 1309–1318.

Warrant, E., Kelber, A., Wcislo, W. T., & Gislén, A., (in preparation). The physiological optics of the compound eyes in the nocturnal bee *Megalopta genalis*.

Warrant, E., & Nilsson, D. (1998). Absorption of white light in photoreceptors. *Vision Research, 38*(2), 195–207.

Warrant, E. J. (2004). Vision in the dimmest habitats on earth. *Journal of Comparative Physiology A, 190*, 765–789.

Warrant, E. J., Porombka, T., & Kirchner, W. (1996). Neural image enhancement allows honey bees to see at night. *Proceedings of the Royal Society of London Series B, Biological Sciences, 263*, 1521–1526.

Wcislo, W. T., Arneson, L., Fernandez, H., Gonzalez, V., Roesch, K., & Smith, A. (2004). The evolution of nocturnal behavior in sweat bees, *Megalopta genalis* and *M. cadoria* (Hymenoptera: Halictidae): An escape from competitors and enemies? *Biological Journal of the Linnean Society, 83*, 377–387.